Frontiers in Bioscience Landmark

Front. Biosci. (Landmark Ed) **2022**; 27(10): 292
https://doi.org/10.31083/j.fbl2710292

Original Research

Nitro-Oxidative Stress and Mitochondrial Dysfunction in Human Cell Lines Exposed to the Environmental Contaminants PFOA and BPA

Maria Chiara Magnifico[1,2,*,†], Marla Xhani[1,3,†], Benedetta Sprovera[1], Brigitta Buttari[4], Giorgia Abballe[1], Flaminia Desideri[1], Emiliano Panieri[5,6], Luciano Saso[5], Marzia Arese[1,*]

[1]Department of Biochemical Sciences "A. Rossi Fanelli", Sapienza University of Rome, 00185 Rome, Italy
[2]Department of Biosciences, Biotechnologies and Biopharmaceutics, University of Bari "Aldo Moro", 70121 Bari, Italy
[3]Istituto Zooprofilattico Sperimentale del Lazio e della Toscana "M. Aleandri", 00178 Rome, Italy
[4]Department of Cardiovascular, Endocrine-Metabolic Diseases and Aging, Italian National Institute of Health, 00161 Rome, Italy
[5]Department of Physiology and Pharmacology "Vittorio Erspamer", Sapienza University of Rome, 00185 Rome, Italy
[6]Section of Hazardous Substances, Environmental Education and Training for the Technical Coordination of Management Activities (DGTEC), Italian Institute for Environmental Protection and Research, 00144 Rome, Italy
*Correspondence: maria.magnifico@uniba.it (Maria Chiara Magnifico); marzia.arese@uniroma1.it (Marzia Arese)
[†]These authors contributed equally.
Academic Editor: Josef Jampílek
Submitted: 26 July 2022 Revised: 13 September 2022 Accepted: 10 October 2022 Published: 27 October 2022

Abstract

Background: Bisphenol A (BPA) and perfluorooctanoic acid (PFOA) are synthetic compounds widely utilized in industrial activities devoted to the production of daily life plastic, metal products, and packaging from which they are able to migrate to food and water. Due to their persistence in the environment, living organisms are chronically exposed to these pollutants. BPA and PFOA have adverse effects on tissues and organs. The aim of this study was to identify the molecular targets and biochemical mechanisms involved in their toxicity. **Methods**: HepG2 and HaCaT cells were treated with BPA or PFOA, and the trypan blue exclusion test and 3-(4,5-Dimethylthiazol-2-yl)-2,5-Diphenyltetrazolium Bromide (MTT) assay were performed to define the conditions for subsequent investigations. We conducted quantitative PCR and western blot analysis to evaluate the expression of proteins involved in nitric oxide (NO) signaling. Cell-based assays were carried out to evaluate reactive oxygen species (ROS) production, nitrite/nitrate (NOx) accumulation, 3-nitrotyrosine (3-NT) formation, and mitochondrial membrane potential (MMP) determination in treated cells. **Results**: HepG2 and HaCaT cells incubated for 24 h with subtoxic concentrations of BPA or PFOA (50 and 10 μM, respectively) exhibited altered mRNA and protein expression levels of NO synthase isoforms, manganese superoxide dismutase, and cytochrome c. Treatment with PFOA led to activation of inducible NO synthase (NOS), a marker of nitrosative stress, accompanied by the increased production of ROS, NOx, and 3-NT and alterations of the MMP compared to controls. **Conclusions**: The results of this study indicate the major involvement of the NO signaling axis in the persistent alteration of cell redox homeostasis and mitochondrial dysfunction induced by BPA and PFOA, highlighting the specific role of PFOA in NOS regulation and induction of nitro-oxidative stress.

Keywords: emerging contaminants; endocrine disruptors; nitric oxide signaling; nitro-oxidative stress; mitochondrial dysfunction

1. Introduction

In healthy cells, the redox balance is maintained through a complex network of adaptive responses that include the continuous generation and elimination of reactive oxygen/nitrogen species (ROS/RNS). The fine-tune regulation of redox signaling events is activated by incoming insults (physical, chemical, or biological) to restore the physiological equilibrium [1–5].

Mitochondria are one of the main endogenous sources of ROS due to the formation of superoxide ion ($O_2^{-\cdot}$) at the level of the electron transport chain [6]. In addition, nitric oxide ($NO\cdot$) production is achieved through the specific activity of NO synthase (NOS) isozymes, i.e., neuronal NOS (nNOS), endothelial NOS (eNOS), and inducible NOS (iNOS) [7,8]. The nNOS and eNOS enzymes catalyze the production of NO needed for signaling [9,10]. By contrast, iNOS activation, characterized by a strong increase in NO concentration (μM), is associated with host defense mechanisms and immune responses [11], but is also responsible for deleterious effects such as the persistent inhibition of oxidative phosphorylation (OXPHOS), redox imbalance, and onset of inflammatory pathways [12–15].

The short-lived, highly reactive peroxynitrite ($ONOO^-$) is generated by the reaction of NO with O_2^- under conditions of increased bioavailability of these substrates. $ONOO^-$ is responsible for the direct or indirect oxidation of biological molecules [16] and for protein modifications occurring at the level of sensitive amino acids, such as the nitrosylation of cysteine and nitration of tyrosine residues [17,18].

A number of xenobiotics and related chemicals (e.g., atmospheric pollutants and industrial contaminants) are involved in the production of intracellular ROS/RNS, and the persistence of a given prooxidant stimulus may specifically

affect redox homeostasis leading to chronic oxidative stress (OS) [4,15].

Diffuse OS is a common alteration in several pathological conditions including hypertension, diabetes, neurodegeneration and cancer [1,6,19,20]. Among the exogenous sources of nitro-OS, there has been growing interest in the chemical derivatives of synthetic compounds utilized in industrial manufacture. These chemicals, widely utilized as plasticizer and waterproof materials for packaging, utensils and pharmaceuticals, are now classified as emerging contaminants (ECs) as they are dispersed in the environment at alarming concentrations [21,22].

Bisphenol A (BPA) and perfluoro-octanoic acid (PFOA) are ideal representatives of this class of pollutants. Due to their intrinsic high stability, resistance to environmental conditions and long half-life, both have been widely used as components of utensils and personal care tools to confer durability, plasticity and impermeabilization [23–25].

The documented migration of BPA and PFOA from products to soil, water and food, and the consequent bioaccumulation of these ECs have established a condition of human chronic exposure to these pollutants through ingestion, inhalation and dermal absorption [26–29]. Great efforts are being made to clarify the adverse effects that both BPA and PFOA may have on living organisms, and to better understand the mechanisms underlying their toxic effects [27,28,30–34].

BPA and PFOA are endocrine disruptors (EDs), i.e., molecules able to interfere with hormone-driven processes [35]. Several studies have shown correlations between exposure to EDs and decreased fertility, as well as an increased incidence of cancers such as breast, ovarian, thyroid, lung, and testis [33,35–38].

Both BPA and PFOA are thought to target the mitochondria of exposed cells, thus inducing mitochondrial dysfunction and promoting an increase of both ROS and RNS with consequent onset of OS [39–43]. Glutamatergic neurons have increased expression of both iNOS and nNOS, resulting in the elevation of ROS and RNS and 3-nitrotyrosine (3-NT) production induced by chronic exposure to BPA [44], whereas 24 h PFOA exposure results in increased ROS and antioxidant enzyme expression in the HepG2 human hepatoma cell line [45]. The proposed mechanisms of BPA and PFOA toxicities are linked to their structural and chemical properties, which favor cell permeability and point to the interactions with hormone receptors (i.e., estrogen receptor and peroxisome proliferator activated receptor alpha, respectively) in exposed cells [46–48]. Recent studies showed that PFOA was able to interact with superoxide dismutase (SOD) directly, inducing OS and apoptosis [49], and may lead to the production of proinflammatory cytokines, ROS/RNS increase and mitochondrial dysfunction in rat cell model [40].

In this work, the mechanisms of toxicity of the EDs BPA and PFOA were investigated, focusing on their ability to interfere with the NO signaling. To this end, two human cell models were chosen to assess the effects of BPA and PFOA treatments: the HepG2 hepatocellular cancer-derived cell line, which is the gold standard model for xenobiotic metabolism and cytotoxicity studies; and the HaCaT immortalized keratinocyte cell line, which is a model system to study the skin as the outer barrier to environmental cytotoxic and genotoxic agents [50–52].

The expression of regulators involved in NO metabolism such as the NOS isoforms (eNOS in HepG2, nNOS in HaCaT and iNOS in both cell lines) was assessed at both the mRNA and protein levels, in association with evaluation of the expression of the mitochondrial proteins manganese SOD (MnSOD) and cytochrome c (cyt c). As a relevant parameter for the analyses of oxidative and nitrosative stress (NS), the level of ROS production in cells treated with BPA and PFOA was determined, as well as the accumulation of nitrites/nitrates (NOx), reflecting the increased production of NO compared to untreated cells. Furthermore, as a downstream effect of altered ROS/RNS homeostasis, we evaluated the level of 3-NT modification in proteins and alterations of the mitochondrial membrane potential (MMP).

Upon cell treatment with low μM concentrations of these substances (50 μM BPA and 10 μM PFOA) the physiologic cell redox homeostasis is affected, with mitochondrial alterations compatible with the onset of a persistent nitro-OS condition.

As members of a wide class of synthetic pollutants (ECs, EDs), both BPA and PFOA have analogues for which a comparable level of toxicity has been reported [27,28,38,39,49]. Further work is needed to clarify the effective EC pressure to which living organisms are exposed and related redox dysregulation is generated. We postulate that a comprehensive understanding of the specific contribution of abundant ECs (e.g., BPA or PFOA) to alterations in NO signaling and the promotion of OS and NS will provide a concrete basis by which to define the harmful effects of these pollutants. Of relevance, the major involvement of NO signaling in the toxicity exerted by the ECs BPA and PFOA and a novel remarkable effect of PFOA on the regulation of NOS isoforms were observed in this study. Within the limitation of the model system (cell lines) and application of selective incubation conditions, which do not represent the complexity of the whole organism, we found this cell line approach as an opportunity to evaluate the parameters related to altered ROS and RNS bioavailability.

The results of this study may provide insight into the effects derived from an impaired antioxidant cell response, which leads to an ROS/RNS increase, bioenergetic dysfunction and inflammation at the tissue level, a condition favoring the onset of pathological states [1,20,53].

2. Materials and Methods

2.1 Cell Culture

The HepG2 human hepatocellular cancer-derived cell line (HB-8065TM; ATCC, Manassas, VA, USA) was maintained in Dulbecco's Modified Eagle Medium (DMEM) supplemented with 2 mM L-glutamine (Aurogene SRL, Rome, Italy), 10% heat-inactivated fetal bovine serum (FBS) and 1% antibiotics of 50 U/mL penicillin and 50 μg/mL streptomycin (both from Aurogene SRL) in a 37 °C, 5% CO_2, 95% air cell culture incubator. The HaCaT human keratinocyte cell line was a kind gift from Professor L. Mosca (Sapienza University of Rome, Rome, Italy); cells were grown at 37 °C, 5% CO_2, 95% air in DMEM containing 4.5 g/L glucose, supplemented with 10% heat inactivated FBS, 2 mM L-glutamine and 50 μg/mL gentamicin (Aurogene SRL) in 25-cm^2 flasks, 75-cm^2 flasks or multiwell plates. The day before the experiments, cells were serum starved in DMEM containing 1 g/L glucose and 2 mM L-glutamine (without FBS, phenol red, or antibiotics).

Cells were incubated in the presence or absence of BPA and PFOA at different concentrations and times. When necessary, cells were harvested by trypsinization and centrifugation (1000 $\times$ g) and carefully suspended in working medium at a density of ~2.8 $\times$ 10^4 cells/cm^2 (HepG2) and ~1.2 $\times$ 10^4 cells/cm^2 (HaCaT). Cells were lysed with Cell Lysis Reagent (CelLytic^{TM} M; Merck Life Science, Darmstadt, Germany) containing protease inhibitor cocktail (Roche, Basel, Switzerland). The BCA assay was used to determine the protein content.

2.2 Chemicals

DMEM and FBS were from Invitrogen Life Technologies (Gibco, Paisley, UK) and PAA Laboratories (Linz, Austria). BPA, perfluorooctanoic acid, JC-1, MTT, and trypan blue solution were from Merck Life Science. PFOA was dissolved in sterile dimethyl sulfoxide (DMSO; Merck Life Science) and further diluted in water; the administration of 10 μM PFOA led to residual DMSO <0.01%. BPA was dissolved in 10% ethanol; the administration of 50 μM BPA led to residual ethanol <0.01%. In the dose-response experiments (Fig. 1) vehicle (0.1% DMSO and 0.02% ethanol) was assayed corresponding to the highest volume of PFOA and BPA administered. Lipopolisaccaride (LPS) from *Escherichia coli* and interferon-γ (IFN-γ) were purchased from Merck Life Science. Nigericin and valinomycin utilized in the MMP determinations were from Abcam (Cambridge, UK).

2.3 Cell Viability Assays

The viability of HepG2 and HaCaT cells was assessed by the trypan blue exclusion test and MTT [3-(4,5-Dimethylthiazol-2-yl)-2,5-Diphenyltetrazolium Bromide] reduction assay as previously described [54]. Briefly, cells seeded on 35 mm dish or 6-well plates were incubated for 24 h with BPA or PFOA (from 1 to 250 μM). After treatment, cells were detached with trypsin, pelleted at 800 $\times$ g, resuspended in phosphate-buffered saline (PBS) and mixed with equal volume of trypan blue. Live (bright clear) and dead (blue) cells were counted in the Thoma cell counting chamber. For the MTT assay, cells (2 $\times$ 10^5/mL) were seeded in a 96-well plate in a final volume of 100 μL/well and in-

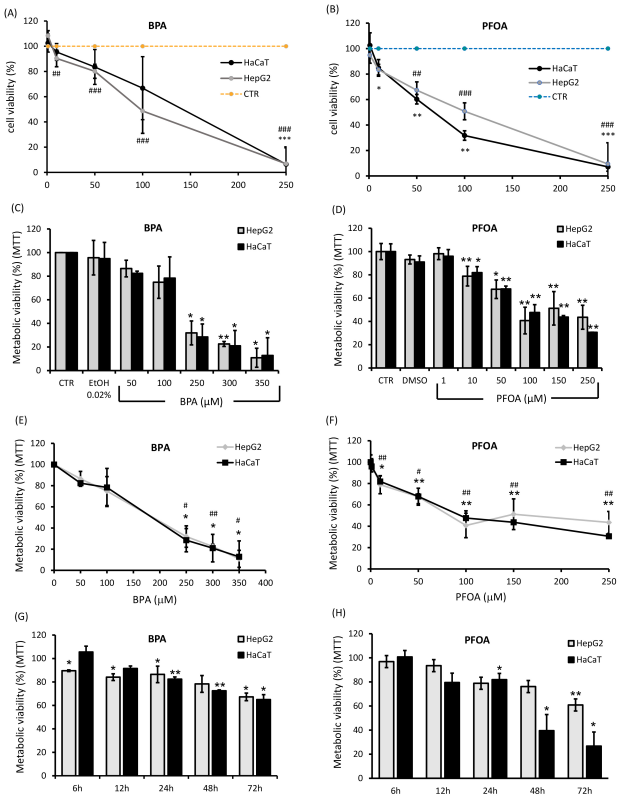

Fig. 1. Viability of HepG2 and HaCaT cells after exposure to BPA and PFOA. The percentage of living cells undergoing treatments with BPA or PFOA was assayed by the trypan blue exclusion test in a concentration range of 0–250 μM (A): BPA; (B) PFOA; # and * indicate the significance of data from HepG2 and HaCaT, respectively. The capacity of cells to reduce MTT was utilized to evaluate cell viability specifically related to mitochondrial integrity and activity (C–H). Dose-response cell viability assays (MTT) were carried out after a 24 h incubation with increasing concentrations of (C) BPA or (D) PFOA; ethanol (0.02%) and DMSO (0.1%) were used as vehicles for BPA and PFOA, respectively. Trends in cell viability decrease from dose-response MTT assays were observed for (E) BPA and (F) PFOA; # and * indicate the significance of data from HepG2 and HaCaT, respectively. Time-course viability of cells (HepG2 and HaCaT) after exposure to (G) 50 μM BPA or (H) 10 μM PFOA as measured by the MTT assay. Data are presented as the percentage of values obtained from untreated cells (100%). Data $\pm$ standard deviation (SD); n $\geq$3. Significance (p values) was assessed by unpaired t-test; $^{\#,*}p \leq 0.05$ *vs* control. $^{\#\#,**}p \leq 0.01$ *vs* control. $^{\#\#\#,***}p \leq 0.001$ vs control.

cubated for 6 to 72 h at 37 °C in the presence or absence of increasing BPA and PFOA concentrations (from 0.1 μM to 1 mM). Then 10 μL MTT solution (5 mg/mL) was added to each well, followed by a 4 h incubation at 37 °C. To dissolve the dark-colored formazan crystals produced by reduction of the MTT tetrazolium salt, cells were incubated for 30 min at 37 °C in the dark with 100 μL DMSO. The optical density of reduced MTT was measured at 570 nm with a reference wavelength at 690 nm using the Appliskan Microplate Reader (Thermo Fisher Scientific, Waltham, MA, USA).

2.4 Quantitative PCR

Quantitative PCR (qPCR) was carried out in HepG2 and HaCaT cells. Briefly, cells were incubated for 24 h with BPA (50 μM) or PFOA (10 μM). After incubation, cells were harvested by trypsinization and centrifugation (1000 $\times$ g for 5 min at 20 °C), washed twice with Hank's buffer and counted. Cells (1×10^6) were lysed in 350 μL RA1 Buffer containing 10 mM DTT, and RNA was isolated and purified using the Nucleo Spin® RNA Kit (Macherey-Nagel, Düren, Germany) according to the manufacturer's instructions. Then, 1 μg total RNA was used for reverse transcription reaction with the RT2 First Strand Kit (Qiagen, Venlo, Netherlands) and qPCR was performed using primers designed by Bio-Rad Laboratories (Hercules, CA, USA) (Software Beacon Designer) and purchased by PrimmBiotech, Cambridge, USA. SYBR Green qPCR (Brilliant_SYBR_Green QPCR Master Mix) was performed using the Stratagene Mx3005p System (both from Agilent Technologies, Santa Clara, CA, USA). The cDNAs were amplified using 45 cycles consisting of a denaturation step (95 °C for 5 min) and amplification step (95 °C for 10 s, 55 °C for 30 s). Melting curve analysis was performed at the end of every run to ensure the presence of a single amplified product for each reaction. The β-actin gene (PrimmBiotech) was used for normalization. The primers used were as follows. nNOS (NOS1) forward: 5′ GCGGTTCTCTATAGCTTCCAGA 3′ reverse: 5′ CCATGTGCTTAATGAAGGACTCG 3′; iNOS (NOS2) forward: 5′ CCGAGTCAGAGTCACCATCC 3′ reverse: 5′ CAGCAGCCGTTCCTCCTC 3′; eNOS (NOS3); forward: 5′ GCCGTGCTGCACAGTTACC 3' reverse: 5′ GCTCATTCTCCAGGTGCTTCAT 3′; MnSOD forward: 5′ TGGCCAAGGGAGATGTTACA 3′ reverse: 5′ TGATATGACCACCACCATTGAAC 3′; cyt c forward: 5′ TTTGGATCCAATGGGTGATGTTGAG 3′ reverse: 5′ TTTGAATTCCTCATTAGTAGCTTTTTTGAG 3′; and β-actin forward: 5′ GCGAGAAGATGACCCAGATC 3′ reverse: 5′ GGATAGCACAGCCTGGATAG 3′.

2.5 Western Blot Analysis

HepG2 and HaCaT cells (3×10^6 cells) were incubated for 24 h with BPA (50 μM), PFOA (10 μM) or untreated, followed by lysis with CellLytic^{TM} M reagent in the presence of protease inhibitors (both from Merck Life Science). Cells were also incubated for 24 h with 1 mg/mL LPS and 10 ng/mL IFN-γ (both from Merck Life Science) as a positive control of iNOS induction. Protein samples (50 μg) were separated on 10% sodium dodecyl sulfate (SDS)-polyacrylamide gel electrophoresis gels and electrotransferred to polyvinylidene difluoride membranes. After blocking for 1.5 h in 4% bovine serum albumin, membranes were incubated overnight at 4 °C with the following primary antibodies: polyclonal anti-iNOS antibody (Boster Biological Technology, Pleasanton, CA, USA), polyclonal anti-eNOS and anti-nNOS antibodies (both from Santa Cruz Biotechnology, Dallas, TX, USA), polyclonal anti-MnSOD antibody (Bio-Rad), monoclonal anti-cyt c antibody (Santa Cruz Biotechnology) and monoclonal anti β-actin antibody (Invitrogen, Waltham, MA, USA). All primary antibodies were diluted 1:1000 in blocking buffer, except anti β-actin antibody that was diluted 1:5000. After washing with PBS/Tween, the membranes were incubated for 1 h at room temperature with horseradish peroxidase-conjugated secondary antibodies (1:5000; Merck Life Science). Proteins were detected with ChemiDocTM MP Image Analysis Software (Bio-Rad) after the addition of Enhanced Chemiluminescence Western Blotting Substrate (Bio-Rad). When necessary, membranes were stripped (in glycine/SDS/Tween 20, pH 2.2) and reprobed with anti-eNOS/nNOS antibodies. Densitometric analysis was carried out with Image Lab 6.0.1 software (Bio-Rad, CA, USA).

2.6 Reactive Oxygen Species Quantification

Reactive oxygen species (ROS) generation was assessed in living cells using two fluorescent probes with a slight difference in ROS specificity for independent evaluations: red-fluorescent MAK145 (Merck Life Science) and 2′,7′-dichlorodihydrofluorescein diacetate (DCFDA) (Cayman Chemical Company, Ann Arbor, MI, USA). Before the assay, HepG2 and HaCaT (~1×10^6 cells/mL) were incubated for 24 h in a 24-well (black) plate in the presence of BPA 50 μM and PFOA 10 μM or untreated; cells were also assayed in the presence of H_2O_2 (0.1 mM) as a positive control. MAK145 was added 1 h before the termination of treatments. After 1 h of incubation, according to the manufacturer's instructions, the fluorescence intensity was measured at λ_{ex} = 520 and λ_{em} = 605 nm. DCFDA (10 μM) was incubated for 30 min at 37 °C after treatment, and the fluorescent signal was measured at λ_{ex} = 485 and λ_{em} = 535 nm. Fluorescence was measured with the VICTOR^{TM} Multilabel Counter Plate Reader (Perkin Elmer, Waltham, MA, USA).

2.7 NOx Determination

The total NOx was evaluated as a quantitative measure of NO production. The accumulation of NOx was assessed in the culture medium of HepG2 and HaCaT cells (~2.5×10^5 cells/mL), which were grown overnight in DMEM 1

g/L glucose (without FBS and phenol red), upon 24 h exposure to BPA 50 μM and PFOA 10 μM. After incubation, the cell supernatants were centrifuged at 1000 $\times$ g for 10 min at 4 °C, and the NOx content was determined fluorometrically using the fluorescent probe 2, 3-diaminonaphthalene (DAN) (Nitrate/Nitrite Fluorometric Assay Kit; Cayman Chemical Company). The fluorescent intensity, which is proportional to total NO production, was measured with the Fluorescence Plate Reader VICTOR Multilabel Counter (Perkin Elmer, Waltham, USA) using an excitation wavelength of 375 nm and emission wavelength of 420 nm.

2.8 Detection of 3-NT Protein Modifications

The evaluation of 3-NT modified proteins was used as marker of peroxynitrite- mediated NS in HepG2 and HaCaT cells treated with BPA 50 μM and PFOA 10 μM or untreated. After treatments, HepG2 cells were trypsinized, centrifuged at 500 $\times$ g for 10 min and washed twice with PBS. The cell pellet (1×10^6 cells) was resuspended with extraction buffer and incubated on ice for 20 min. After centrifugation at 12000 $\times$ g 4 °C for 20 min, the 3-NT levels were assessed colorimetrically using the competitive Nitrotyrosine ELISA Kit (Abcam) and normalized to the total protein content determined by the BCA assay. The absorbance was measured at 450 nm using the Appliskan Microplate Reader (Thermo Fisher Scientific).

2.9 MMP Measurements

MMP was measured by flow cytometry (Accuri C6 Flow Cytometer®; Becton Dickinson, Franklin Lakes, NJ, USA) to detect the accumulation of the cationic fluorescent probe JC-1 (5,5',6,6'-tetrachloro-1,1',3,3' tetraethylbenzimidazolylcarbocyanine iodide) (Abcam) into the mitochondrial negatively charged matrix according to the manufacturer's instructions [55]. Briefly, after treatment with BPA 50 μM or PFOA 10 μM, HepG2 and HaCaT cells were trypsinized, pelleted at 1000 $\times$ g for 5 min at 20°C, and resuspended in PBS at a density of 5×10^5 cells/mL. Cell suspensions were incubated for 20 min in the dark with JC-1 2.5 μg/mL, washed twice and resuspended in 300 μL PBS. When necessary, 0.6 μM nigericin was added. After the addition of nigericin, the fluorescence level peaked within approximately 20 min; thereafter, the fluorescence signal was rapidly dissipated with the addition of 0.2 μM valinomycin. JC-1 was excited at 488 nm, green fluorescence was quantified at 530 nm (FL1 channel), and red fluorescence was quantified at 585 nm (FL2 channel).

2.10 Statistical Analyses

Data are reported as the mean $\pm$ standard deviation of at least three independent experiments and significance (p values) were determined using the unpaired Student's t-test. $p \leq 0.05$ was considered statistically significant.

3. Results

3.1 Cytotoxicity of BPA and PFOA in HepG2 and HaCaT cells

The cytotoxicity of BPA and PFOA in HepG2 and HaCaT cells was determined by the trypan blue exclusion and MTT assays (Fig. 1). Dose-response analyses were performed by incubating both cell lines with increasing amounts of BPA or PFOA. As shown in Fig. 1A–C, 24 h exposure to BPA induced similar effects on HaCaT and HepG2 cells, namely, a decrease in cell viability of about 20% in a concentration range of 50–100 μM, followed by an additional decrease in viability of about 50% at a BPA concentration of 250 μM. After further increasing the BPA concentration, higher toxicity was observed, leading to residual viability of ~20% in both HaCaT and HepG2 cell lines. Dose-response analyses after the administration of PFOA revealed a 20% decrease in the viability of both cell lines at 10 μM, followed by an additional decrease at 50 μM PFOA (~70% overall viability) (Fig. 1B,D). In a concentration range of 100–250 μM PFOA, the overall decreasing trend observed was more pronounced for HaCaT than HepG2 cells. To better analyze the sensitivity of HaCaT and HepG2 cells to BPA/PFOA and to identify the condition of sublethal toxicity suitable for further investigations, the MTT assay was conducted for the time-dependent evaluation of the effects exerted by the ECs (Fig. 1G,H). At a concentration of 50 μM for BPA or 10 μM for PFOA, the overall cell metabolic activity was within a 20% value, and a decrease in cell viability was observed as a function of time. Extended exposure to BPA of both cell lines (Fig. 1E) resulted in a further ~10% decrease of metabolically active cells, reaching 70% after 72 h. A similar trend was observed after extending the PFOA incubation time, and slightly higher sensitivity was observed in HaCaT cells compared to HepG2 cells, with the former displaying a marked decrease in cell viability (30% viable cells) compared to the latter (60% viable cells) after 72 h of PFOA treatment (Fig. 1F).

The results of the viability assays allowed us to identify a suitable concentration and incubation time for further experiments: 50 μM for BPA or 10 μM PFOA, for 24 h. These conditions were indeed considered subtoxic, accounting for the limited metabolic alteration observed (within 20%).

3.2 NOS Isoform Expression in HepG2 and HaCaT Cells Exposed to BPA and to PFOA

The mRNA and protein levels of the different isoforms of NOS (iNOS and tissue-specific NOS, eNOS produced in hepatocytes [HepG2], and nNOS expressed in keratinocytes [HaCaT]) were determined after incubation with BPA or PFOA for 24 h. Compared to controls, BPA induced a two-fold increase in both iNOS ($p = 0.015$ *vs* ctr) and eNOS ($p = 0.023$ *vs* ctr) mRNA in HepG2 cells; the effect of PFOA on iNOS activation was higher (four-fold; $p =$

6×10^{-4} *vs* ctr), but differently from BPA, PFOA weakly decreased eNOS mRNA (less than 10%) (p = 0.0022 *vs* ctr) (Fig. 2A). In parallel, in HaCaT cells, BPA treatment resulted in increased mRNA expression of both NOS isoforms (Fig. 2B), but the effect was limited to a 1.5-fold increase (p = iNOS 0.054; p = nNOS 0.016 in HaCaT cells) compared to HepG2 cells. Similar to that observed in HepG2 cells, PFOA induced a significant decrease in nNOS mRNA in keratinocytes (~25%; p = 0.047 *vs* ctr), whereas iNOS was significantly upregulated (~1.4-fold; p = 0.017 *vs* ctr). The protein expression of the two NOS isoforms in HepG2 cells was consistent with the changes in mRNA expression, with a maximum increase of 50% upon PFOA treatment (p iNOS $_{BPA}$ = 0.026 *vs* ctr; p eNOS $_{BPA}$ = 0.013 BPA *vs* ctr; p iNOS $_{PFOA}$ = 6.1 $\pm$ 10^{-5} *vs* ctr); p eNOS = 0.013 BPA *vs* ctr) compared to controls (Fig. 2C). A similar increase with respect to iNOS expression was observed after 24 h cell treatment with a mixture of IFN-γ and LPS (p = 0.0067 *vs* ctr), a positive control of iNOS induction (Fig. 2C). NOS protein detected by Western blotting in HaCaT cells showed iNOS increase above 1.5-fold (p = 0.017 *vs* ctr) upon PFOA treatment, whereas the effect of BPA on iNOS induction was only very small although significant (~10%; p = 0.026 *vs* ctr) (Fig. 2E). nNOS production was found to be comparable with the control level (Fig. 2E) after the various treatments, except for a narrow but significant increase (20%; p = 0.014 *vs* ctr) induced by BPA (Fig. 2E). The effect of PFOA on NOS protein expression was reproducible in the cell line assayed, with iNOS induction as a specific target.

3.3 MnSOD and cyt c Expression in HepG2 and HaCaT Cells Exposed to BPA and to PFOA

The mRNA expression levels of the mitochondrial proteins MnSOD and cyt c were detected following treatment of HepG2 and HaCaT cells with BPA or PFOA under the conditions previously described. The level of MnSOD mRNA was not significantly altered in HepG2 after 24 h of BPA exposure, and was slightly induced by PFOA (1.25-fold; p = 0.014 *vs* ctr) (Fig. 3A), although at the protein level, the significant upregulation of MnSOD was induced by both EDs (40% BPA increase; p $_{BPA}$ = 0.02 *vs* ctr; 60% PFOA increase; p $_{PFOA}$ = 1.7 $\times$ 10^{-5} *vs* ctr), as shown in Fig. 3B. In HaCaT cells, a ~two-fold increment in MnSOD expression was induced by PFOA at mRNA level (p = 0.018 *vs* ctr) (Fig. 3C). Furthermore, the protein expression detected by anti-MnSOD antibody was increased by both BPA (40% increment; p = 0.019 *vs* ctr) and PFOA (34% increment; p = 2.1 $\times$ 10^{-6} *vs* ctr) (Fig. 3D), similar to what was observed in HepG2 cells under comparable incubation conditions.

The analysis of cyt c expression showed mRNA induction specifically driven by PFOA treatment of both cell lines, with a stronger effect observed in HepG2 cells (above two-fold, p = 0.0036; Fig. 4A) compared to Ha-

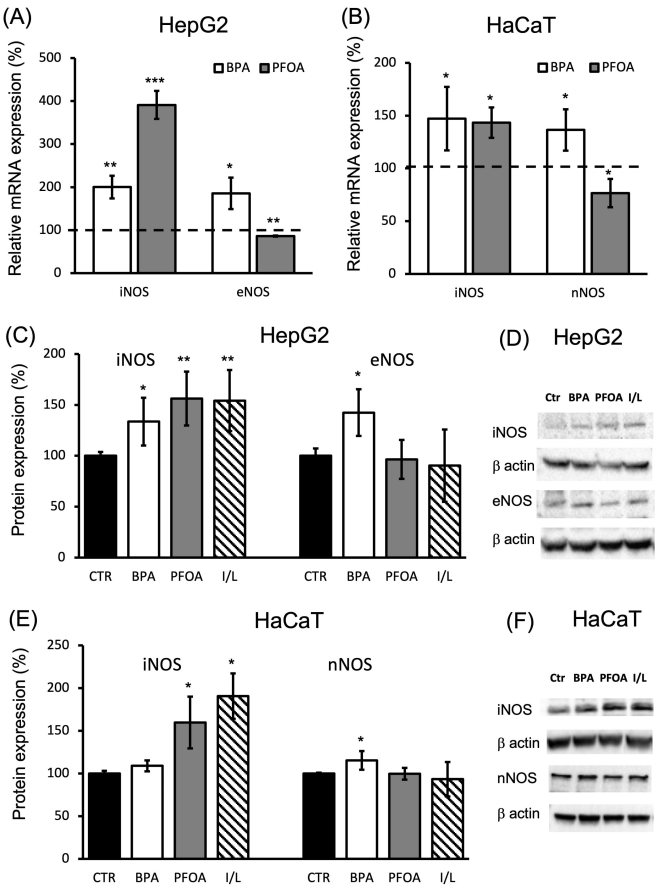

Fig. 2. NOS isoform expression in HepG2 cells and HaCaT cells treated with BPA or PFOA. (A–B) qPCR analysis was carried out (A) in the presence of iNOS/eNOS specific primers and cDNA purified from HepG2 cells treated for 24 h with 50 μM BPA (white bars) or 10 μM PFOA (grey bars); (B) in the presence of iNOS/nNOS specific primers and cDNA isolated from HaCaT cells after treatments. Data are reported as the percentage with respect to the expression of untreated cells. β actin was used as the reference gene. (C–F) NOS isoform protein expression detected by Western blot analysis with specific antibodies in cell lysates after BPA (white lanes) or PFOA (grey lanes) treatment: (C) analysis of iNOS and eNOS proteins in HepG2 and (D) corresponding enhanced chemiluminescence (ECL) bands (E): iNOS and nNOS protein levels in HaCaT lysates, (F) corresponding ECL bands. Data are presented as the percentage with respect to untreated cells (black bars); 24 h IFN-γ (10 ng/mL) + LPS (1 mg/mL) treatment was assayed as a positive control of iNOS induction (I/L, zebrine bars); Bands were detected by ECL after hybridization with peroxidase-conjugated secondary antibodies; densitometric analysis was conducted with Image Lab software with β actin expression taken as reference in each sample (see methods and **Supplementary Materials** for details). Data $\pm$ SD.; n $\geq$3. Significance (p values) was assessed by unpaired t-test; *$p \leq 0.05$ *vs* control. **$p \leq 0.01$ *vs* control. ***$p \leq 0.001$ *vs* Control.

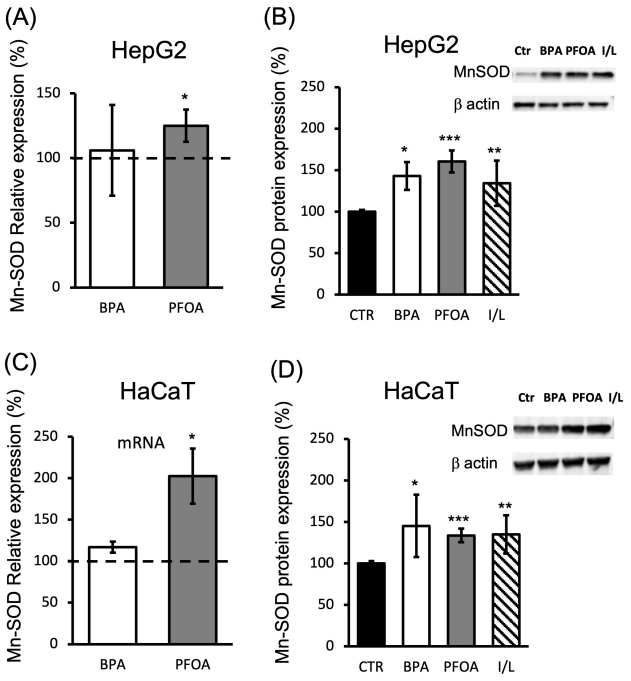

Fig. 3. MnSOD expression in HepG2 and HaCaT cells treated with BPA and PFOA. (A,C) MnSOD mRNA evaluation by qPCR analysis was carried out in the presence of MnSOD-specific primers (see methods) and cDNA purified from (A) HepG2 or (C) HaCaT cells treated for 24 h with 50 μM BPA (white) or 10 μM PFOA (gray) lanes; data are reported as percentage with respect to the expression of untreated cells. β actin was used as the reference gene. (B,D) MnSOD protein expression detected by Western blotting conducted with anti-MnSOD antibody after 24 h treatments (see above); (B) HepG2, (D) HaCaT cells; data are presented as percentage with respect to untreated cells (black lanes); I/L: 24 h IFN-γ + LPS treatment (zebrine lanes); insets: MnSOD western blot bands detected by ECL (see **Supplementary Material** for details). Data $\pm$ SD; n $\geq$3. Significance (p values) was assessed by unpaired t-test; *$p \leq 0.05$ *vs* control; **$p \leq 0.01$ *vs* control; ***$p \leq 0.001$ *vs* control.

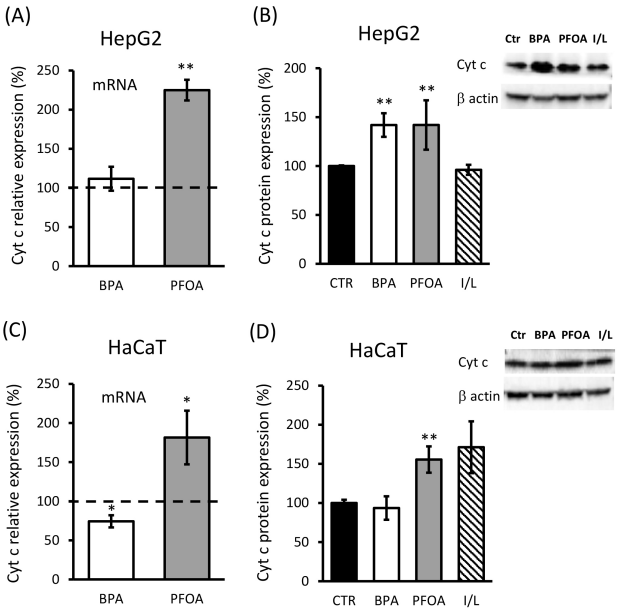

Fig. 4. Cyt c expression in HaCaT cells treated with BPA and PFOA. (A,C) Cyt c mRNA evaluation by qPCR analysis carried out in the presence of cyt c-specific primers (see methods) and cDNA purified from (A) HepG2 or (C) HaCaT cells treated for 24 h with 50 μM BPA (white) or 10 μM PFOA (gray) lanes; data are reported as the percentage with respect to the expression of untreated cells. β actin was used as the reference gene. (B,D) Cyt c protein expression detected by Western blotting carried out with anti-cyt c antibody after 24 h treatments (see above); (B) HepG2 and (F) HaCaT cells; data are presented as the percentage with respect to untreated cells (black lanes); I/L: 24 h IFN-γ + LPS treatment (zebrine lanes); inset: cyt c western blot bands detected by ECL (see **Supplementary Material** for details). Data $\pm$ SD; n $\geq$3. Significance (p values) was assessed by unpaired t-test; *$p \leq 0.05$ *vs* control; **$p \leq 0.01$ *vs* control.

CaT (~1.8-fold, $p = 0.045$; Fig. 4C). BPA treatment led to a small but significant decrease in cyt c mRNA (35% decrease; $p = 0.036$), with the effect limited to HaCaT cells, as in HepG2 cells, there was no significant change in cyt c mRNA expression after BPA treatment compared to the control (Fig. 4A). As shown in Fig. 4B, cyt c protein expression detected by Western blot analysis in HepG2 cells was ~1.4-fold higher in response to both BPA ($p = 0.0087$) and PFOA ($p = 0.01$) treatment, whereas the response of HaCaT cells regarding cyt c protein expression (Fig. 4D) was reproduced only in the case of PFOA treatment (~1.5-fold increase; $p = 0.0013$) but not by BPA. In keratinocytes, indeed, BPA led to no changes in cyt c protein expression under the condition assayed.

Overall, in HaCaT cells, 24 h treatment with BPA showed a lower sensitivity in terms of cyt c and MnSOD expression with respect to HepG2 and compared with the effects exerted by PFOA.

3.4 ROS, NOx, and 3-NT Induction by BPA and PFOA

The production of ROS, the accumulation of NOx and the amount of NT modifications in proteins (3-NT) were measured to assess the OS and NS levels in HepG2 and HaCaT cells after 24 h treatment with BPA or PFOA. ROS determination was carried out taking advantage of two different ROS-targeting probes, for independent evaluations: DCFDA (Fig. 5A), mainly targeting hydrogen peroxide (H_2O_2) but with broad sensitivity towards other ROS and RNS, such as peroxynitrite; and the MAK-145 red-fluorescent probe (Fig. 5B) with selectivity for superoxide and hydroxyl radicals. Under the conditions assayed (24 h incubation with 50 μM BPA or 10 μM PFOA), ROS levels were specifically increased to ~50% with respect to control values as revealed by the DCFDA assay (Fig. 5A). Specif-

ically, BPA induced a ~40% ROS increase in HaCaT (p = 0.006 *vs* ctr) but not HepG2 cells, whereas PFOA treatment induced a similar increase in both HepG2 (45% increase; p = 0.0117 *vs* ctr) and HaCaT (50% increase; p = 0.045 *vs* ctr) cells. IFN-γ + LPS and H_2O_2 were used as positive controls. A much lower ROS level was detected by the MAK-145 probe, with significance in the case of BPA treatment of HepG2 cells (20%; p = 0.043 *vs* ctr) but not in HaCaT cells (p = 0.55 *vs* ctr). A small but significant ROS induction was also observed upon PFOA treatment of HepG2 (27%; p = 0.025) and HaCaT (32%; p = 0.041) cells compared to controls (Fig. 5B).

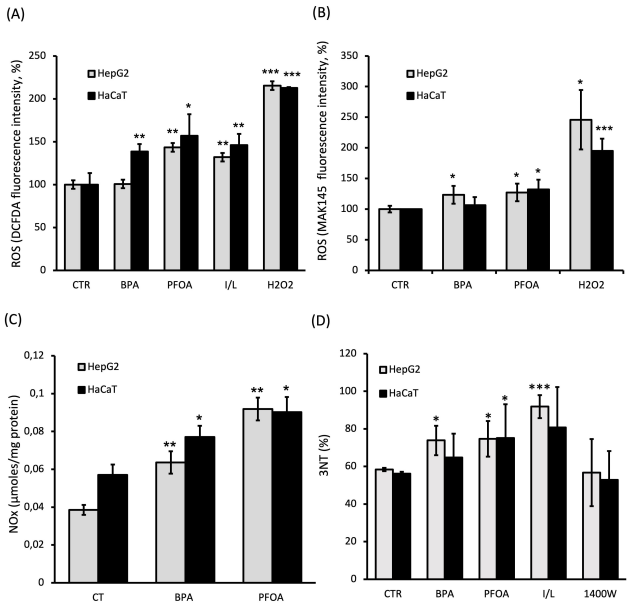

Fig. 5. OS and NS induced by BPA and PFOA. Assays were carried out following 24 h incubation of both HaCaT and HepG2 cells with BPA 50 μM or PFOA 10 μM. (A,B) Intracellular ROS levels measured in HepG2 and HaCaT cells in the presence of (A) DCFDA and (B) red fluorescent MAK145 ROS-targeting probes (see methods). Data are presented as the percentage of values obtained from untreated cells and normalized for protein content. Data are the mean $\pm$ SD; n = 3. * $p \leq 0.05$ *vs* control; ** $p \leq 0.01$ *vs* control; *** $p \leq 0.001$ *vs* control. (C) NOx accumulation (24 h) quantified from cell supernatant by DAN as described in the Methods section. Data $\pm$ SD; n = 3. * $p \leq 0.05$ *vs* control; ** $p \leq 0.01$ *vs* control. (D) 3-NT determination. Protein 3-NT modifications detected by NT competitive ELISA (see methods) in BPA- or PFOA-treated and untreated cells (lysate). Data are the mean $\pm$ SD; n = 3. Significance (p values) was assessed by unpaired t-test; * $p \leq 0.05$ *vs* control; ** $p \leq 0.01$ *vs* control; *** $p \leq 0.001$ *vs* control. Exact p values are in the main text.

The levels of NO end products, NOx, were found to be increased by treatment with both BPA and PFOA in the two cell lines tested (Fig. 5C). The effect was more evident in PFOA-treated cells, resulting in the increased accumulation of NOx by about two-fold and 1.5-fold for HepG2 (p = 0.0012) and HaCaT (p = 0.05) cells, respectively. A smaller but clearly significant induction of NOx was also achieved by BPA, by about 1.5-fold in both cell lines (p HepG2 = 0.009 and p HaCaT = 0.045 *vs* controls). It is worth noting that the result of increased NOx accumulation was in good agreement with the observation of increased NOS expression (especially iNOS) observed upon ED treatments.

As shown in Fig. 5D, the amount of NT modification in proteins was increased of about 25% in HepG2 cells following treatment of both BPA (p = 0.029 *vs* ctr) and PFOA (p = 0.018 *vs* ctr). Similar changes were seen in HaCaT cells exposed to PFOA (p = 0.021 *vs* ctr), whereas only a small irrelevant increase was observed for BPA (lower than 20%) under the assayed conditions. It is worth mentioning that a 24 h incubation of IFN-γ/LPS was able to specifically raise NO concentration in cells by iNOS activation, leading to the highest NT level, whereas the iNOS inhibitor 1400W showed the lowest level of NT, comparable in average to the control.

3.5 MMP of BPA- and PFOA-Treated HepG2 and HaCaT Cells

The overall mitochondrial functional state was investigated by measuring the MMP of BPA- or PFOA-treated cells, by evaluating the mitochondrial import of the fluorescent probe JC-1 and the formation of the red J-aggregates. As shown in Fig. 6A, after 24 h incubation with BPA, the MMP was significantly lowered in HepG2 (~20% decrease; p = 0.0115) and HaCaT (~40% decrease; p = 0.023), whereas no significant difference was induced by PFOA. Surprisingly, the response of the MMP to the two-step addition of the ionophores nigericin and valinomycin, indicated a condition of hyperpolarization determined by the incubation of cells with PFOA. The hyperpolarization was significant in HepG2 (~30% decrease; p = 0.032) with respect to the polarization level of the untreated cells, whereas a small non-significant depolarization was observed for BPA treatment (Fig. 6B). The MMP alterations described, specifically induced by BPA or PFOA, were observed in the two cell lines assayed.

4. Discussion

Environmental diffusion of the ECs BPA and PFOA, compounds widely utilized in industrial manufacturing processes [21,22], has resulted in alarming concentrations detected in water and soil as well as bioaccumulation, as demonstrated by the detection of both BPA and PFOA in human body fluids with documented mother to fetus transfer [56,57]. The adverse effects exerted by chronic exposure of BPA and PFOA have been described over the last several years [27,32,35]. Of relevance, the ED action shown for both compounds [33,35,36], and related alterations of the physiological hormonal signals are strictly

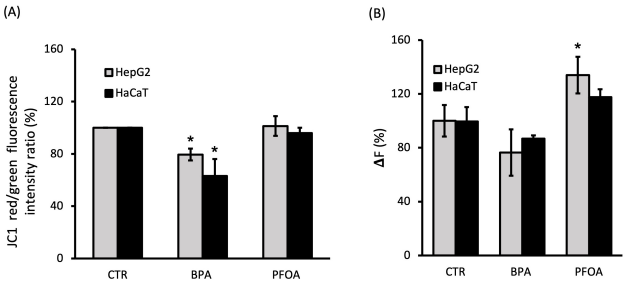

Fig. 6. MMP in cells incubated with BPA and PFOA. (A) The percentage of intensity ratio between red and green fluorescence of JC-1 was measured by flow cytometry in HepG2 and HaCaT cells after 24 h incubation with BPA 50 μM or PFOA 10 μM. (B) MMP of cells incubated for 24 h with BPA 50 μM or PFOA 10 μM. $\triangle$F value (% of control) calculated as the difference between the maximal fluorescence of JC-1 reached after the addition of 0.6 μM nigericin (Nig) and the fluorescence measured after the addition of 0.2 μM valinomycin (Val). Val was added (at plateau) to collapse the membrane potential. Data $\pm$ SD, $n = 3$. Significance (p values) was assessed by unpaired *t*-test; * $p \leq 0.05$ *versus* control. Exact *p* values are reported in the main text.

connected to the perturbation of cellular pathways related to redox homeostasis. The involvement of BPA in OS induction has been previously suggested based on its interaction with estrogen receptors, although the mechanisms of this process need to be elucidated [27,31,41,44,58].

This paper reports a detailed characterization of the biochemical parameters related to OS and NS induced by BPA, showing a correlation between alterations of ROS and RNS signaling and establishment of a cell redox imbalance with consequences at the mitochondrial level. Furthermore, the novelty of the specific involvement of PFOA in the perturbation of the NO signaling axis is proposed here, with activation of iNOS and production of peroxinitrite, suggesting a specific effect exerted by PFOA toward NS induction, under the condition assayed.

The limitations of the study with respect to the biomedical relevance of the findings must be taken into account, with particular reference to the cell models and the concentration of ECs assayed. As transformed/immortalized cells, the HepG2 and HaCaT cell lines utilized in this study may display altered metabolism and viability respect to normal cells. However, it must be considered that the cell lines utilized represent a model system for toxicological studies and that the experimental condition utilized (low glucose adaptation, FBS and phenol red starvation) were adopted to minimize eventual deviations in the results. The screening of dose-response and time dependency of the ECs carried out by the trypan blue exclusion test and MTT assay (Fig. 1) was conducted to establish a suitable concentration and time window for further investigations regarding OS and NS in cell models of interest.

At the concentrations of 50 μM BPA or 10 μM PFOA, only minor effects were observed on cell viability ($\leq$20%; Fig. 1A–F), whereas the same doses led to specific induction of mRNA encoding for the iNOS enzyme, with stronger effects exerted by PFOA (four-fold iNOS induction in HepG2 cells) with respect to BPA (two-fold iNOS induction in HepG2 cells). BPA was able to induce a significant effect in terms of a "physiological" NOS (eNOS/nNOS) modulation, whereas PFOA failed to evoke this specific cell response (Fig. 2A,B). These considerations can be extended to the protein level (Fig. 2C–F), as the increase in iNOS and e/nNOS showed a trend consistent with the mRNA data, although a smaller amplitude of the effect (1.6-fold average increase) was observed, and with a relevant exception given by the absence of iNOS induction in HaCaT cells by BPA. These observations strongly suggest that both BPA and PFOA have the ability to specifically affect the NO signaling axis, although through different mechanisms.

The increased expression of the "physiological" tissue-specific NOS isoform (eNOS in HepG2 and nNOS in HaCaT) induced by BPA may indicate the activation of adaptation pathways that possibly stimulated a specific cell stress response counteracting the detrimental activity of iNOS to limit the increase of highly reactive molecules to an acceptable range in terms of OS/NS. Under the condition assayed (50 μM, 24 h), in agreement with a previous observation, BPA incubation was associated with increases in MnSOD protein expression (Fig. 3). A parallel induction of cyt c expression was observed in HepG2 BPA-treated cells (Fig. 4), whereas HaCaT was insensitive to BPA with respect to cyt c stimulation. The variation in ROS level observed was generally small in amplitude (Fig. 5A,B), in accordance with an increase in MnSOD activity. In the case of BPA treatment, ROS were almost comparable with untreated cells, except for a 1.5-fold increase in HaCaT detected by DCFDA, which may possibly be associated with less evident MnSOD activation in that cell line (Fig. 3D). The increase in NO end products induced by BPA in both cell lines was in agreement with activation of the NO signaling axis (Fig. 5C). These results were in line with an increase in 3-NT protein modifications observed in BPA-treated HepG2 cells, although the results were not significant in HaCaT cells (Fig. 5D). In keratinocytes, the analysis of data arising from BPA treatments would seem indicative of their lower sensitization to this toxic compound; however, these results are possibly related to a cell response compatible with a different time window with respect to the condition assayed, as suggested by the increase in ROS production observed after 1–4 h treatment with BPA (not shown).

At the mitochondrial level, BPA administration led to a decrease in MMP in both cell lines (Fig. 6A). In HaCaT cells, this result was associated with the low involvement of cyt c with respect to BPA-induced modulatory events

(Fig. 4C,D), revealing a depressed mitochondrial function. In view of the endocrine disruptive activity of BPA, under the conditions herein explored, we clearly showed that alteration of the NO axis [43,44] and dysregulation of the mitochondrial parameters [41], which have been previously proposed, are indeed strictly correlated and may be associated with the induction of nitro-OS [31,33].

The results observed upon PFOA treatment (10 μM, 24 h) showed the activation of iNOS at both the mRNA (four-fold increase in HepG2 cells) and protein (60% increase) levels. Differently from BPA, this effect was not associated to a parallel increase of the physiological NOS isoform, but iNOS induction was accompanied by a small but significant decrease in eNOS and nNOS mRNA in HepG2 and HaCaT cells, respectively (Fig. 2A,B). The observation of the specific effect of PFOA on NO signaling is novel, and is related to the documented inverse "crosstalk" occurring among the NOS isoforms under specific cell conditions approaching the onset of NS [15]. The increase of iNOS expression induced by PFOA led the inducible isoform to prevail over eNOS, suggesting the onset of a more severe level of oxidative and nitrosative damage induced by PFOA with respect to BPA, especially in hepatocytes, where the effects of long-lasting NO increase derived by iNOS activity might trigger the initiation of inflammation. The modulatory trend among NOS isoforms observed at the mRNA level and confirmed at the protein expression level was associated with the increment in OS and NS markers, such as ROS production, NOx accumulation, and 3-NT protein modification (Fig. 5A–D). The results discussed above with respect to HepG2 cells exposed to PFOA were only partially reproduced in HaCaT cells, where the same treatment was able to only induce a more confined but still significant iNOS activation (Fig. 2B) confirmed by NOx accumulation, which was not associated with a substantial increase in 3-NT-specific damage. In both cell lines, PFOA treatment was able to induce a small but significant increase in MnSOD expression under the conditions assayed (Fig. 3), a result that, as mentioned above, may possibly explain the general finding of a limited increase in ROS levels compared to controls (Fig. 5A,B). However, the evidence of a consistent increment in DCFDA-targeted ROS detected in HepG2 cells might be due to the sensitivity of DCFDA for RNS and associated with an NS-specific induction driven by PFOA in HepG2 cells. Focusing on mitochondrial functional parameters, PFOA was able to induce a significant increase in mitochondrial potential, as indicated by the increased $\Delta\psi$ component of the MMP observed in the presence of ionophores (Fig. 6B). It is worth noting that the observed mitochondrial hyperpolarization specifically induced by PFOA was associated with increased cyt c expression (Fig. 4A,B) suggesting a degree of inhibition at the OXPHOS level. The results presented point to an association between alteration of mitochondrial function and OS, and highlight the role of the NS component generated through activation of the NO-axis to the overall degree of cell dysfunction induced by both EDs, particularly PFOA.

5. Conclusions

BPA and PFOA are both able to influence and alter the NO signaling pathway and promote the alteration of mitochondrial function. In hepatocytes, PFOA determines a proinflammatory condition, characterized by the high level of iNOS expression, increased ROS, significant alteration of proteins at the nitro-tyrosine level, and mitochondrial hyperpolarization. In the same cells, BPA was active in deregulating physiologic eNOS/iNOS crosstalk at the expression level, leading to elevation of NT modification with consequences at the mitochondrial level, as suggested by the decreased MMP. The keratinocyte response to insult arising from contaminant administration in the case of PFOA resulted in lower involvement of NO signaling compared to HepG2, but still with indications of an altered MMP and MnSOD activation at the mitochondrial level. The observed (mild) induction of iNOS mRNA driven by BPA was not accompanied by increased iNOS protein in keratinocytes, with the overall effect of a minor involvement of the NO axis under the tested conditions. However, BPA was able to induce persistent mitochondrial depolarization in keratinocytes, in accordance with the endocrine-disruption physiological alterations induced by this compound.

The experimental work herein presented shows that BPA and PFOA may target different components of the NO signaling pathway, with downstream effects mostly related to alteration of cell redox homeostasis. Further investigations are needed to fully understand the bioenergetic alterations and cell response linked to the nitro-OS induced by these pollutants. The findings reported will help clarify the mechanisms of action of BPA and PFOA, which will aid in the management of pathological relapses linked to chronic exposure to these environmental contaminants.

Abbreviations

3-NT, 3-nitrotyrosine; BCA, Bicinchoninic acid; BPA, Bisphenol A; Cyt c, Cytochrome c; DAN, 1,1',3,3'-tetraethyl-5,5',6,6'-tetrachloroimidacarbocyanine iodide; DCFDA, dichlorodihydrofluorescein diacetate; DMSO, Dimethyl sulfoxide; DTT, Dithiothreitol; ECs, Emerging contaminants; EDs, Endocrine Disruptors; eNOS, Endothelial nitric oxide synthase; ER, Estrogen receptor; iNOS, Inducible nitric oxide synthase; JC-1, 1,1',3,3'-tetraethyl-5,5',6,6'-tetrachloroimidacarbocyanine iodide; MMP, Mitochondrial membrane potential; MnSOD, Manganese superoxide dismutase; MTT, 3(4,5-dimethylthiazol-2-yl)-2,5-diphenyltetrazolium bromide; nNOS, Neuronal nitric oxide synthase; NO, Nitric oxide; NOx, Nitrogen oxides; OS, Oxidative stress; OXPHOS, Oxidative phosphorylation; PFOA, Perfluoro-octanoic acid; qPCR, Quantitative PCR Reaction; RNS, Reactive nitrogen species; ROS, Reactive oxygen species; SOD, Superoxide dismutase.

Author Contributions

MCM and MA designed the research study. MX, BS, GA and FD performed the research. MCM and BS analyzed the data. MA, MCM and BB wrote the manuscript. EP and LS provided advice on data finalization and supervised manuscript preparation. All authors contributed to editorial changes in the manuscript. All authors read and approved the final manuscript.

Ethics Approval and Consent to Participate

Not applicable.

Acknowledgment

We warmly acknowledge Prof. Paolo Sarti (Department of Biochemical Science "A. Rossi Fanelli", Sapienza University of Rome) for promoting and supporting this project. Dr. Mario Carere (Department of Environment and Health, Istituto Superiore di Sanità, Rome, Italy) is acknowledged for fruitful discussion and methodological advices on environmental pollutants. Prof. Luciana Mosca (Department of Biochemical Science "A. Rossi Fanelli", Sapienza University of Rome) is gratefully acknowledged for providing us the HaCaT cell line.

Funding

Work supported by Regione Lazio of Italy (FILAS-RU-2014-1020 to prof. Paolo Sarti). Sapienza Progetti di Ateneo to M.A. RP11715C819AF6BA. Ph.D. fellowship of M.Xh. was funded by the Enrico and Enrica Sovena Foundation (Italy).

Conflict of Interest

Luciano Saso is serving as one of the Guest Editors of the special issue "Modulation of oxidative stress: Biochemical and pharmacological aspects", in this journal. We declare that Luciano Saso had no involvement in the peer review of this article and has no access to information regarding its peer review. Full responsibility for the editorial process of this article was delegated to Josef Jampílek.

Apart from what is mentioned above, all the authors declare that there is no conflict of interest.

Supplementary Material

Supplementary data related to Fig. 1 (exact the *p* values of the dose-response and time-dependence experiments) and Figs. 2,3,4 (Western blot) are available. Supplementary material associated with this article can be found, in the online version, at https://doi.org/10.31083/j.fbl2710292.

References

[1] Valko M, Leibfritz D, Moncol J, Cronin MTD, Mazur M, Telser J. Free radicals and antioxidants in normal physiological functions and human disease. The International Journal of Biochemistry & Cell Biology. 2007; 39: 44–84.

[2] Matthijnssens J, Ciarlet M, Rahman M, Attoui H, Estes MK, Gentsch JR, *et al*. Redox-based regulation of signal transduction: principles, pitfalls, and promises. Free Radical Biology and Medicine. 2009; 153: 1621–1629.

[3] Dröge W. Free Radicals in the Physiological Control of Cell Function. Physiological Reviews. 2002; 82: 47–95.

[4] Rahal A, Kumar A, Singh V, Yadav B, Tiwari R, Chakraborty S, *et al*. Oxidative Stress, Prooxidants, and Antioxidants: the Interplay. BioMed Research International. 2014; 2014: 1–19.

[5] Mirończuk-Chodakowska I, Witkowska AM, Zujko ME. Endogenous non-enzymatic antioxidants in the human body. Advances in Medical Sciences. 2018; 63: 68–78.

[6] Lenaz G. Mitochondria and reactive oxygen species. Which role in physiology and pathology? Advances in Experimental Medicine and Biology. 2012; 942: 93–136.

[7] Forstermann U, Sessa WC. Nitric oxide synthases: regulation and function. European Heart Journal. 2012; 33: 829–837.

[8] Moncada S, Bolanos JP. Nitric oxide, cell bioenergetics and neurodegeneration. Journal of Neurochemistry. 2006; 97: 1676–1689.

[9] Ignarro LJ, Buga GM, Wei LH, Bauer PM, Wu G, Del Soldato P. Role of the arginine-nitric oxide pathway in the regulation of vascular smooth muscle cell proliferation. Proceedings of the National Academy of Sciences of the United States of America. 2001; 98: 4202–4208.

[10] Garthwaite J. From synaptically localized to volume transmission by nitric oxide. The Journal of Physiology. 2016; 594: 9–18.

[11] Xue Q, Yan Y, Zhang R, Xiong H. Regulation of iNOS on immune cells and its role in diseases. International Journal of Molecular Sciences. 2018; 19: 3805.

[12] Clementi E, Brown GC, Feelisch M, Moncada S. Persistent inhibition of cell respiration by nitric oxide: Crucial role of S-nitrosylation of mitochondrial complex I and protective action of glutathione. Proceedings of the National Academy of Sciences of the United States of America. 1998; 95: 7631–7636.

[13] Cinelli MA, Do HT, Miley GP, Silverman RB. Inducible nitric oxide synthase: Regulation, structure, and inhibition. Medicinal Research Reviews. 2020; 40: 158–189.

[14] Magnifico MC, Oberkersch RE, Mollo A, Giambelli L, Grooten Y, Sarti P, *et al*. VLDL Induced Modulation of Nitric Oxide Signalling and Cell Redox Homeostasis in HUVEC. Oxidative Medicine and Cellular Longevity. 2017; 2017: 1–15.

[15] Magnifico MC, Xhani M, Popov M, Saso L, Sarti P, Arese M. Nonylphenol and Octylphenol Differently Affect Cell Redox Balance by Modulating the Nitric Oxide Signaling. Oxidative Medicine and Cellular Longevity. 2018; 2018: 1–13.

[16] Radi R. Peroxynitrite, a Stealthy Biological Oxidant. Journal of Biological Chemistry. 2013; 288: 26464–26472.

[17] Bartesaghi S,Radi R. Fundamentals on the biochemistry of peroxynitrite and protein tyrosine nitration. Redox Biology. 2018; 14: PMC5694970.

[18] Janssen-Heininger YMW, Mossman BT, Heintz NH, Forman HJ, Kalyanaraman B, Finkel T, *et al*. Redox-based regulation of signal transduction: Principles, pitfalls, and promises. Free Radical Biology and Medicine. 2008; 45: 1–17.

[19] Wang R, Geller DA, Wink DA, Cheng B, Billiar TR. No and hepatocellular cancer. British Journal of Pharmacology. 2019; 177: 5459–5466.

[20] Pérez-Torres I, Manzano-Pech L, Rubio-Ruíz ME, Soto ME, Guarner-Lans V. Nitrosative stress and its association with cardiometabolic disorders. Molecules. 2020; 25: 2555.

[21] Wilkinson JL, Hooda PS, Barker J, Barton S, Swinden J. Ecotoxic pharmaceuticals, personal care products, and other emerging contaminants: a review of environmental, receptor-mediated, developmental, and epigenetic toxicity with discus-

sion of proposed toxicity to humans. Critical Reviews in Environmental Science and Technology. 2016; 46: 336–381.
[22] Koch A, Kärrman A, Yeung LWY, Jonsson M, Ahrens L, Wang T. Point source characterization of per- And polyfluoroalkyl substances (PFASs) and extractable organofluorine (EOF) in freshwater and aquatic invertebrates. Environmental Science: Processes & Impacts. 2019; 21: 1887–1898.
[23] Stahlhut RW, Welshons WV, Swan SH. Bisphenol A data in NHANES suggest longer than expected half-life, substantial nonfood exposure, or both. Environmental Health Perspectives. 2009; 117: 784–789.
[24] Lindstrom AB, Strynar MJ, Libelo EL. Polyfluorinated Compounds: Past, Present, and Future. Environmental Science & Technology. 2011; 45: 7954–7961.
[25] Li Y, Fletcher T, Mucs D, Scott K, Lindh CH, Tallving P, *et al*. Half-lives of PFOS, PFHxS and PFOA after end of exposure to contaminated drinking water. Occupational and Environmental Medicine. 2018; 75: 46–51.
[26] Liao C, Kannan K. A survey of alkylphenols, bisphenols, and triclosan in personal care products from China and the United States. Archives of Environmental Contamination and Toxicology. 2014; 67: 50–59.
[27] Andújar N, Gálvez-Ontiveros Y, Zafra-Gómez A, Rodrigo L, Álvarez-Cubero MJ, Aguilera M, *et al*. Bisphenol A analogues in food and their hormonal and obesogenic effects: A review. Nutrients. 2019; 11: 2136.
[28] Wang H, Liu Z hua, Zhang J, Huang RP, Yin H, Dang Z. Human exposure of bisphenol A and its analogues: understandings from human urinary excretion data and wastewater-based epidemiology. Environmental Science and Pollution Research. 2020; 27: 3247–3256.
[29] Göckener B, Weber T, Rüdel H, Bücking M, Kolossa-Gehring M. Human biomonitoring of per- and polyfluoroalkyl substances in German blood plasma samples from 1982 to 2019. Environment International. 2020; 145: 106123.
[30] Welshons W V., Nagel SC, Vom Saal FS. Large effects from small exposures. III. Endocrine mechanisms mediating effects of bisphenol A at levels of human exposure. Endocrinology. 2006; 147: S56–S69.
[31] Gassman NR. Induction of oxidative stress by bisphenol a and its pleiotropic effects. Environmental and Molecular Mutagenesis. 2017; 58: 60–71.
[32] Li K, Gao P, Xiang P, Zhang X, Cui X, Ma LQ. Molecular mechanisms of PFOA-induced toxicity in animals and humans: Implications for health risks. Environment International. 2017; 99: 43–54.
[33] Acconcia F, Pallottini V, Marino M. Molecular mechanisms of action of BPA. Dose-Response. 2015; 13: 1559325815610582.
[34] Gebreab KY, Eeza MNH, Bai T, Zuberi Z, Matysik J, O'Shea KE, *et al*. Comparative toxicometabolomics of perfluorooctanoic acid (PFOA) and next-generation perfluoroalkyl substances. Environmental Pollution. 2020; 265: 114928.
[35] Papalou O, Kandaraki EA, Papadakis G, Diamanti-Kandarakis E. Endocrine disrupting chemicals: An occult mediator of metabolic disease. Frontiers in Endocrinology. 2019; 10: 112.
[36] Saejia P, Lirdprapamongkol K, Svasti J, Paricharttanakul NM. Perfluorooctanoic Acid Enhances Invasion of Follicular Thyroid Carcinoma Cells through NF-κB and Matrix Metalloproteinase-2 Activation. Anticancer Research. 2019; 39: 2429–2435.
[37] Zhang KS, Chen HQ, Chen YS, Qiu KF, Zheng X Bin, Li GC, *et al*. Bisphenol A stimulates human lung cancer cell migration via upregulation of matrix metalloproteinases by GPER/EGFR/ERK1/2 signal pathway. Biomedicine & Pharmacotherapy. 2014; 68: 1037–1043.
[38] Siracusa JS, Yin L, Measel E, Liang S, Yu X. Effects of bisphenol A and its analogs on reproductive health: A mini review. Reproductive Toxicology. 2018; 79: 96–123.
[39] Xu M, Liu G, Li M, Huo M, Zong W, Liu R. Probing the Cell Apoptosis Pathway Induced by Perfluorooctanoic Acid and Perfluorooctane Sulfonate at the Subcellular and Molecular Levels. Journal of Agricultural and Food Chemistry. 2020; 68: 633–641.
[40] Suh KS, Choi EM, Kim YJ, Hong SM, Park SY, Rhee SY, *et al*. Perfluorooctanoic acid induces oxidative damage and mitochondrial dysfunction in pancreatic β-cells. Molecular Medicine Reports. 2017; 15: 3871–3878.
[41] Wang C, He J, Xu T, Han H, Zhu Z, Meng L, *et al*. Bisphenol A(BPA), BPS and BPB-induced oxidative stress and apoptosis mediated by mitochondria in human neuroblastoma cell lines. Ecotoxicology and Environmental Safety. 2021; 207: 111299.
[42] Wang Q, Chen W, Zhang B, Gao Z, Zhang Q, Deng H, *et al*. Perfluorooctanoic acid induces hepatocellular endoplasmic reticulum stress and mitochondrial-mediated apoptosis in vitro via endoplasmic reticulum-mitochondria communication. Chemico-Biological Interactions. 2022; 354: 109844.
[43] Oguro A, Sugitani A, Kobayashi Y, Sakuma R, Imaoka S. Bisphenol a stabilizes Nrf2 via Ca2+ influx by direct activation of the IP3 receptor. Journal of Toxicological Sciences. 2021; 46: 1–10.
[44] Wang H, Chang L, Aguilar JS, Dong S, Hong Y. Bisphenol-a exposure induced neurotoxicity in glutamatergic neurons derived from human embryonic stem cells. Environment International. 2019; 127: 324–332.
[45] Abudayyak M, Öztaş E, Özhan G. Determination of Perflouorooctanoic Acid Toxicity in a Human Hepatocarcinoma Cell Line. Journal of Health and Pollution. 2021; 11: 210909.
[46] Wetherill YB, Akingbemi BT, Kanno J, McLachlan JA, Nadal A, Sonnenschein C, *et al*. *In vitro* molecular mechanisms of bisphenol A action. Reproductive Toxicology. 2007; 24: 178–198.
[47] Klaunig JE, Hocevar BA, Kamendulis LM. Mode of Action analysis of perfluorooctanoic acid (PFOA) tumorigenicity and Human Relevance. Reproductive Toxicology. 2012; 33: 410–418.
[48] Santoro A, Chianese R, Troisi J, Richards S, Nori SL, Fasano S, *et al*. Neuro-toxic and Reproductive Effects of BPA. Current Neuropharmacology. 2019; 17: 1109–1132.
[49] Xu M, Wan J, Niu Q, Liu R. PFOA and PFOS interact with superoxide dismutase and induce cytotoxicity in mouse primary hepatocytes: A combined cellular and molecular methods. Environmental Research. 2019; 175: 63–70.
[50] Mersch-Sundermann V, Knasmüller S, Wu X, Darroudi F, Kassie F. Use of a human-derived liver cell line for the detection of cytoprotective, antigenotoxic and cogenotoxic agents. Toxicology. 2004; 198: 329–340.
[51] Chen Y, Liu X, Wang H, Liu S, Hu N, Li X. Akt regulated phosphorylation of GSK-3β/cyclin D1, p21 and p27 contributes to cell proliferation through cell cycle progression from G1 to S/G2M phase in low-dose arsenite exposed HaCaT cells. Frontiers in Pharmacology. 2019; 10: 1176.
[52] Boukamp P, Petrussevska RT, Breitkreutz D, Hornung J, Markham A, Fusenig NE. Normal keratinization in a spontaneously immortalized aneuploid human keratinocyte cell line. The Journal of Cell Biology. 1988; 106: 761–771.
[53] Tang X, Luo YX, Chen HZ, Liu DP. Mitochondria, endothelial cell function, and vascular diseases. Frontiers In Physiology. 2014; 5 MAY: 1–17.
[54] Hansen J, Bross P. A Cellular Viability Assay to Monitor Drug Toxicity. Methods in Molecular Biology. 2010; 7: 303–311.
[55] Cossarizza A, Baccaranicontri M, Kalashnikova G, Franceschi C. A New Method for the Cytofluorometric Analysis of Mitochondrial Membrane Potential Using the J-Aggregate Forming Lipophilic Cation 5,5′,6,6′-Tetrachloro-1,1′,3,3′-

tetraethylbenzimidazolcarbocyanine Iodide (JC-1). Biochemical and Biophysical Research Communications. 1993; 197: 40–45.

[56] Jin H, Xie J, Mao L, Zhao M, Bai X, Wen J, *et al*. Bisphenol analogue concentrations in human breast milk and their associations with postnatal infant growth. Environmental Pollution. 2020; 259: 113779.

[57] Bell EM, Yeung EH, Ma W, Kannan K, Sundaram R, Smarr MM, *et al*. Concentrations of endocrine disrupting chemicals in newborn blood spots and infant outcomes in the upstate KIDS study. Environment International. 2018; 121: 232–239.

[58] Huang M, Liu S, Fu L, Jiang X, Yang M. Bisphenol A and its analogues bisphenol S, bisphenol F and bisphenol AF induce oxidative stress and biomacromolecular damage in human granulosa KGN cells. Chemosphere. 2020; 253: 126707.